JOURNAL OF GEOPHYSICAL RESEARCH, VOL. 115, A07316, doi:10.1029/2010JA015324, 2010

Click Here for Full Article

Zonal drift of plasma particles inside equatorial plasma bubbles and its relation to the zonal drift of the bubble structure

Chao-Song Huang,[1] O. de La Beaujardiere,[2] R. F. Pfaff,[3] J. M. Retterer,[2] P. A. Roddy,[2] D. E. Hunton,[2] Y.-J. Su,[2] S.-Y. Su,[4] and F. J. Rich[5]

Received 1 February 2010; revised 1 March 2010; accepted 12 March 2010; published 17 July 2010.

[1] It has been observed that the zonal drift velocity of equatorial plasma bubbles is generally eastward. However, it has not been well understood whether the zonal drift of plasma bubbles is the same as the ambient plasma drift and what process causes differences in the drift velocities of the ambient plasma and bubbles. In this study we analyze the ion drift velocities measured by the Defense Meteorological Satellites Program and ROCSAT-1 satellites and the electric fields measured by the Communications/Navigation Outage Forecasting System (C/NOFS) satellite in the presence of equatorial spread *F*. We find that the zonal drift velocity of the plasma particles inside plasma bubbles is significantly different from the ambient plasma drift. The relative zonal velocity of the ions inside the depletion region with respect to the ambient plasma is generally westward. In most cases it can be as high as several hundreds of meters per second. The plasma bubbles detected by the C/NOFS satellite in the midnight-dawn sector are still growing, and the polarization electric field inside the postmidnight bubbles is much stronger than the electric field in the ambient plasma. We suggest that the zonal drift velocity of the plasma particles inside the depletion region is driven by polarization electric field. When a plasma bubble is tilted, the $\mathbf{E} \times \mathbf{B}$ drift velocity caused by the polarization electric field has an upward component and a zonal component. Because of the zonal motion of the plasma particles inside the bubble, the eastward drift velocity of the bubble structure is faster than the ambient plasma drift for a west-tilted bubble and slower than the ambient plasma drift for an east-tilted bubble.

Citation: Huang, C.-S., O. de La Beaujardiere, R. F. Pfaff, J. M. Retterer, P. A. Roddy, D. E. Hunton, Y.-J. Su, S.-Y. Su, and F. J. Rich (2010), Zonal drift of plasma particles inside equatorial plasma bubbles and its relation to the zonal drift of the bubble structure, *J. Geophys. Res.*, *115*, A07316, doi:10.1029/2010JA015324.

1. Introduction

[2] Large-scale plumelike structures in the nighttime equatorial ionosphere were first detected by the Jicamarca incoherent scatter radar and are often associated with equatorial spread *F* (ESF) [*Woodman and La Hoz*, 1976; *Kelley et al.*, 1981]. Numerical simulations reproduced the generation and evolution of equatorial plumes [*Scannapieco and Ossakow*, 1976; *Zalesak et al.*, 1982; *Huang and Kelley*, 1996a, 1996b, 1996c; *Keskinen et al.*, 2003; *Huba et al.*, 2008; *Retterer et al.*, 2009; *Retterer*, 2010]. It has been well understood that the plumes represent depleted plasma density structures and are generated through the Rayleigh-Taylor instability. The plasma instability is excited in the bottomside *F* region and evolves nonlinearly into density depletions that penetrate the *F* peak to the topside *F* region. Because the plasma density inside the depleted regions can be reduced by 2–3 orders of magnitude, the structure of the depletions is often termed plasma bubble. In this paper we analyze the zonal drift of plasma particles inside plasma bubbles and its relation to the zonal drift of the bubble structure.

[3] Plasma bubbles drift in the zonal direction. *Abdu et al.* [1985] found that the bubble structures drift eastward at night and westward in the early morning, and the reversal of the zonal drift velocity occurs around 0400 LT. *Valladares et al.* [1996] identified eastward drifts of equatorial spread *F* irregularities in the evening sector and westward drifts in the postmidnight sector from ionospheric scintillations. *Taylor et al.* [1997] reported that the zonal drift of plasma depletions reverses around midnight. *Abdu et al.* [2003] found a case in which the zonal drift velocity of the plasma bubbles was initially very low eastward and then turned into steadily increasing westward velocity that lasted till early

[1]Boston College, Institute for Scientific Research, Chestnut Hill, Massachusetts, USA.
[2]Air Force Research Laboratory, Hanscom AFB, Massachusetts, USA.
[3]NASA Goddard Space Flight Center, Greenbelt, Maryland, USA.
[4]Institute of Space Science and Center for Space and Remote Sensing Research, National Central University, Chung-Li, Taiwan.
[5]Lincoln Laboratory, Massachusetts Institute of Technology, Lexington, Massachusetts, USA.

Copyright 2010 by the American Geophysical Union.
0148-0227/10/2010JA015324

morning hours. *Yokoyama et al.* [2004] reported observations of the zonal drift of radar backscatter plumes associated with ESF. All irregularity echoes in their cases began to appear at sunset time, growing rapidly and drifting eastward. *Immel et al.* [2003, 2004] and *Park et al.* [2007] analyzed the distribution of the FUV emissions of the equatorial airglow bands associated with the ESF depletions observed by the Imager for Magnetospheric-to-Aurora Global Exploration (IMAGE) satellite. They found that the zonal drift velocity of the plasma depletions derived from the image data is eastward and depends on geomagnetic and solar activity, as well as on season and longitude.

[4] The Jicamarca radar measurements show that the average zonal drift of the equatorial ionospheric *F* region plasma is eastward at night and becomes westward near dawn [*Fejer et al.*, 1991, 2005]. The zonal drift velocity of the plasma depletions and its variation with local time are similar to those of the average *F* region plasma drift [*Abdu et al.*, 1985, 2003; *Valladares et al.*, 1996; *Taylor et al.*, 1997; *Sobral et al.*, 1999; *Immel et al.*, 2003, 2004; *Park et al.*, 2007]. It was suggested that the depletions are embedded in the surrounding plasma and that the zonal drift velocity of the depletions can be used as an indicator of the ambient plasma drift. The reversal of the zonal drift of depletions from eastward to westward around midnight could be caused by disturbance dynamo effects because of enhanced geomagnetic activity.

[5] However, it is important to point out that the zonal drift velocity presented in these studies is the drift velocity of the plasma depletions; no simultaneous measurement of the background plasma drift was made in these experiments. In fact, some investigators have noticed the difference between the average *F* region plasma zonal drift and the zonal drift of plasma depletions. *Valladares et al.* [1996] mentioned that the average scintillation drifts were generally larger than the average incoherent scatter drifts. *Bhattacharyya et al.* [2001] found that the motion of the ESF irregularities was highly variable in the initial phase of irregularity development and suggested that the estimated drifts of the irregularities should not be considered as representative of the ambient plasma drift until ~2200 LT. *Immel et al.* [2003] showed that the plasma depletion drift velocities observed by IMAGE-FUV were 10–50 m s^{-1} higher than the average plasma drift velocities recorded by the Jicamarca incoherent scatter radar, with the largest differences at early local times. *Lin et al.* [2005] compared the simultaneous observations of the IMAGE and ROCSAT-1 satellite data and found that the zonal drift of the plasma bubbles was faster than the ambient plasma drift. The outstanding problems are whether the zonal drift of depletions is indeed different from the ambient plasma drift and, if yes, what causes the different drift velocities of the depletions and ambient plasma.

[6] In this study we analyze the ion drift velocities measured by the Defense Meteorological Satellites Program (DMSP) and ROCSAT-1 satellites and the electric fields measured by the Communications/Navigation Outage Forecasting System (C/NOFS) satellite during ESF processes. Our study focuses on the following critical issues: What are the characteristics of the drift velocities of plasma particles inside plasma bubbles? What determines the drift velocities of the plasma particles? What is the relation between the zonal drift of the plasma particles inside a bubble and the zonal drift of the bubble structure? We will propose a mechanism that can explain the different zonal drift velocities of the ambient plasma and depletions.

2. Observations

[7] We first present the measurements of the DMSP F12 and F15 satellites in the evening equatorial ionosphere. We use the thermal plasma data obtained with the Special Sensor for Ion, Electrons, and Scintillation [*Rich and Hairston*, 1994] on board the DMSP spacecraft. The DMSP F12 and F15 spacecraft are in a polar orbit at a geocentric altitude of ~840 km and cross the equatorial region at 2030 and 2100 MLT, respectively. We choose the cases that occurred during the solar maximum year of 2000. In these cases the background oxygen ion density in the evening equatorial ionosphere was generally higher than 2×10^5 cm^{-3}, the oxygen ion density inside plasma bubbles was higher than 1×10^4 cm^{-3}, and the ion density at the altitude of the DMSP orbit consisted almost completely of oxygen ions (>98%). The high ion density and predominant O^+ fraction guarantee that the ion velocity measurements are reliable.

[8] Figure 1a shows the ion density, ion vertical velocity, and ion zonal velocity measured by the DMSP F15 spacecraft over low latitudes on 29 February 2000. Considering that the ion velocity measurement may have an offset, we do not try to get the absolute value of the ambient plasma drift velocity from the DMSP data. Instead, we analyze the relative velocity of the plasma particles inside the density depletion region with respect to the ambient plasma (the plasma outside the depletion region). We take the velocity at the edge of the depletion to be zero. If the velocity at the leading edge is different from that at the trailing edge, the velocity at the leading edge is taken to be zero. In other words, only the velocity difference between the depletion region and the outside plasma is plotted for the DMSP ion velocity data.

[9] In Figure 1a, the density depletion occurs between −8° and 5° magnetic latitudes. The yellow shading denotes the region with large ion drift velocities. Actually, there are two velocity peaks: one is located at about −5° and the other is at about 2°. The ion vertical velocity inside the depletion region is upward, showing that the depletion is a rising plasma bubble. The ion zonal velocity is negative, indicating that the plasma particles inside the depletion region drift westward. The maximum upward and westward velocities reach 400 m s^{-1}. Figure 1b presents another example in which the ion drift velocities show the same characteristics. The important feature is that the zonal drift velocity of the plasma particles inside the depletion region is significantly different from the ambient plasma drift.

[10] We searched the DMSP data over January–March 2000 and found 530 cases of plasma density depletions at low latitudes in the evening sector. In these 530 cases, the ion zonal velocity inside the depletion region relative to the ambient plasma is westward in 399 cases (75%), small or near zero in 101 cases (19%), and eastward in only 30 cases (6%). We are not going to conduct a statistical analysis in this paper. What we want to address is that the zonal drift of the ions inside depletion regions is westward in an absolute majority of plasma depletions. Previous studies show that the background plasma and depletions drift eastward in the evening sector. If we assume that the ambient plasma also drifts eastward in our cases, the DMSP observations, such as

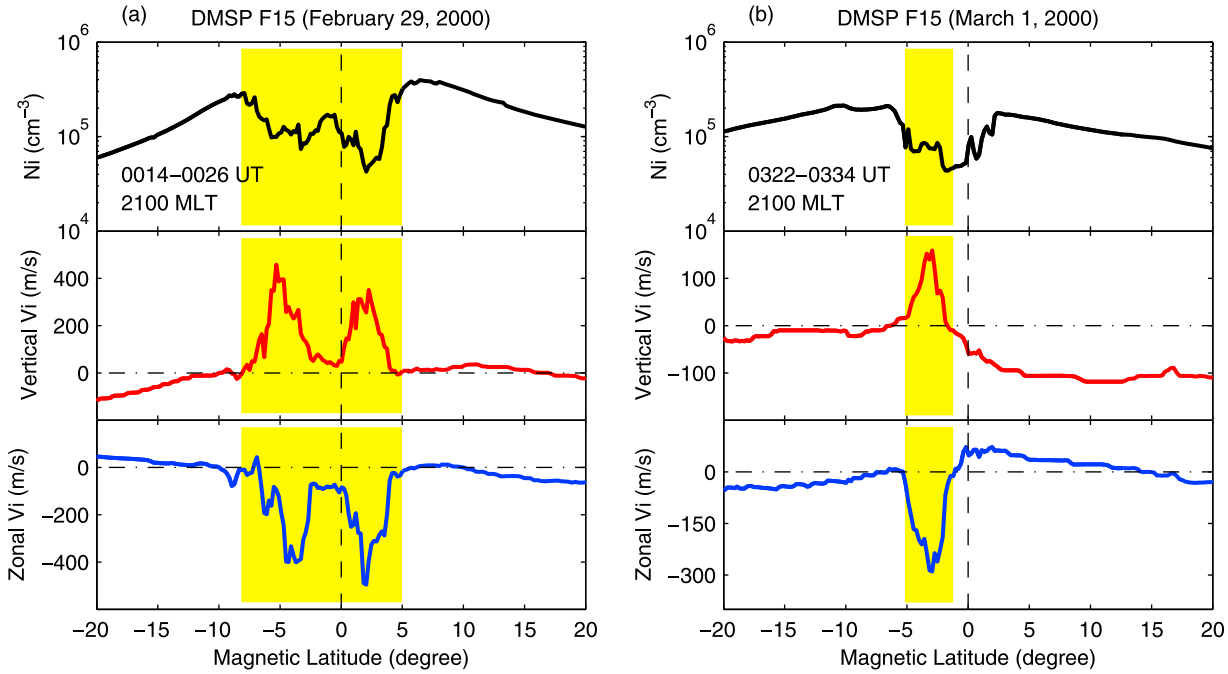

Figure 1. Examples of westward drift of plasma particles inside the density depletion region. From top to bottom show the ion density, ion vertical velocity, and ion zonal velocity measured by the DMSP F15 satellite on (a) 29 February and (b) 1 March 2000. The zonal velocity is positive in the eastward direction and negative in the westward direction.

those displayed in Figure 1, suggest that the zonal drift of the plasma particles inside depletions is generally opposite to the ambient plasma drift.

[11] We next present four examples in which the ion zonal drift inside depletions is eastward or shows complicated characteristics. In Figure 2, the yellow shading denotes the westward ion drift, and the gray shading denotes the eastward ion drift. The ion vertical velocity is upward in all cases, indicating that the plasma bubbles are rising. In the case of Figure 2a, the ion zonal drift inside the depletion is strongly eastward in the region of large upward velocity and becomes weakly eastward in the region of small upward velocity. The ion zonal velocity is more complex in the cases of Figures 2b–2d. The variation of the ion zonal velocity can be eastward-westward (Figure 2b), westward-eastward-westward (Figure 2c), and eastward-westward-eastward (Figure 2d). The observations reveal that the plasma particles drift eastward in some portion of the depletion region and westward in other portion.

[12] Here we give a brief explanation of how the eastward-westward ion drift is defined in our statistics. If the eastward ion velocity inside the depletions is larger than the westward ion velocity, the case is classified in the category of eastward drift. Besides the case of Figure 2a, the cases of Figures 2b–2d are all put into this category because of the dominant eastward drift inside the depletion regions. It should be mentioned that the four cases of Figure 2 are used to display the different characteristics of the ion zonal drift inside depletions. In fact, the ion zonal drift inside depletions has similar large eastward component in only ~6% of the total cases.

[13] We have also found that the ion zonal drift inside depletion regions can be very close to the ambient plasma drift in a number of cases. Two examples are presented in Figure 3. The yellow shading denotes the density depletion region. In these cases, both the vertical and zonal ion drifts inside the depletions are nearly the same as those outside the depletion region. Because the plasma particles inside the depletions are no longer moving upward, such depletions can be considered as dead bubbles. The zonal drift of the plasma particles inside dead bubbles is nearly the same as the ambient plasma drift.

[14] We now present two cases in which plasma depletions were detected by the DMSP and ROCSAT-1 satellites nearly simultaneously. The altitudes of the DMSP and ROCSAT-1 satellites are ~840 km and ~600 km, respectively. The ROCSAT-1 data have a time resolution of 1 s. Potential offset in the ion drift velocity of the ROCSAT-1 measurements has been removed, and the ion velocity in the ROCSAT-1 data represents the real velocity rather than the relative velocity with respect to the ambient plasma.

[15] Figure 4a shows the ion density, ion vertical velocity, and ion zonal velocity measured by ROCSAT-1 between 2132 and 2140 UT on 3 March 2000. Local time (LT), geographic longitude, and magnetic latitude are listed at the bottom of Figure 4. Five plasma density depletions are detected in the evening sector during this period, as denoted by the shaded intervals. The ion vertical velocity is upward in all the depletions, implying that the depletions are rising plasma bubbles. The zonal drift velocity of the ambient plasma outside the depletion regions is positive, indicating that the ambient plasma is drifting eastward. In contrast, the zonal drift velocity of the ions inside the depletion regions is significantly different from the ambient plasma drift and can be eastward or westward. Figure 4b presents the DMSP F15 measurements of the plasma depletion only a few minutes

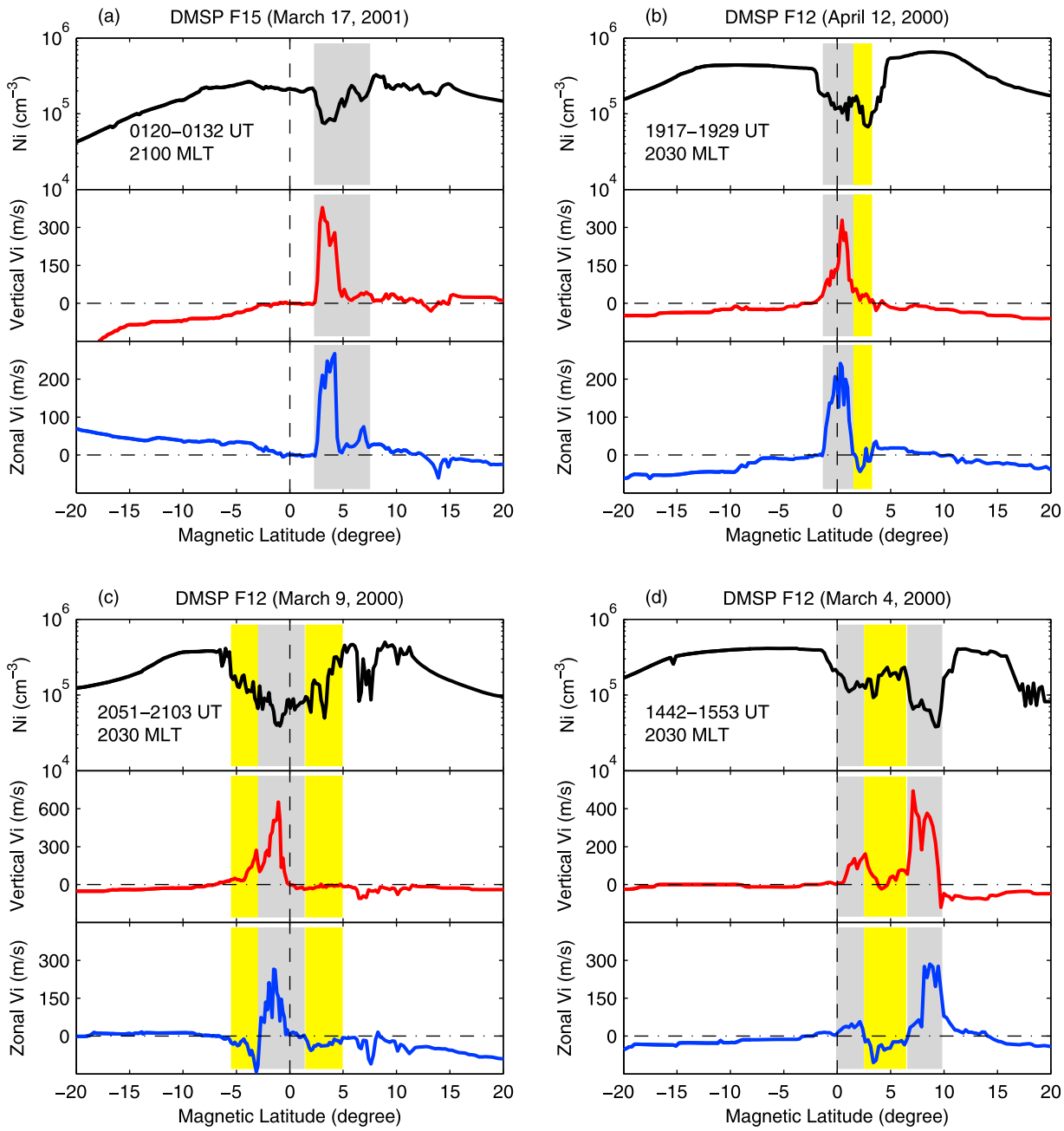

Figure 2. Examples of eastward-westward drifts of plasma particles inside the density depletion region. From top to bottom show the ion density, ion vertical velocity, and ion zonal velocity measured by the DMSP F15 or F12 satellite on (a) 17 March, (b) 12 April, (c) 9 March, and (d) 4 March 2000. The zonal velocity is positive in the eastward direction and negative in the westward direction.

later. The local time, longitude, and latitude of F15 are very close to those of ROCSAT-1. The ion zonal drift in the depletion region shows eastward-westward variations. The measurements of ROCSAT-1 and F15 suggest that multiple plasma bubbles occurred in this case. However, because the F15 measurements were not exactly at the same location and time as the ROCSAT-1 measurements, it is not certain whether the plasma bubble detected by F15 was one of the bubbles detected by ROCSAT-1. Figures 4c–4d present the data of the ROCSAT-1 and DMSP F12 satellites in another case. The F12 measurement is ~15 min later than the ROCSAT-1 measurement. All features of the ion drift velocities in the case of Figures 4c–4d are similar to those in the case of Figures 4a–4b.

[16] In the cases of Figure 4, the ambient plasma drift is eastward in the evening sector, but the zonal drift of the plasma particles inside the depletion regions can be eastward or westward. The difference between the ambient plasma drift and the ion drift inside the depletions can be as high as hundreds of meters per second. These characteristics

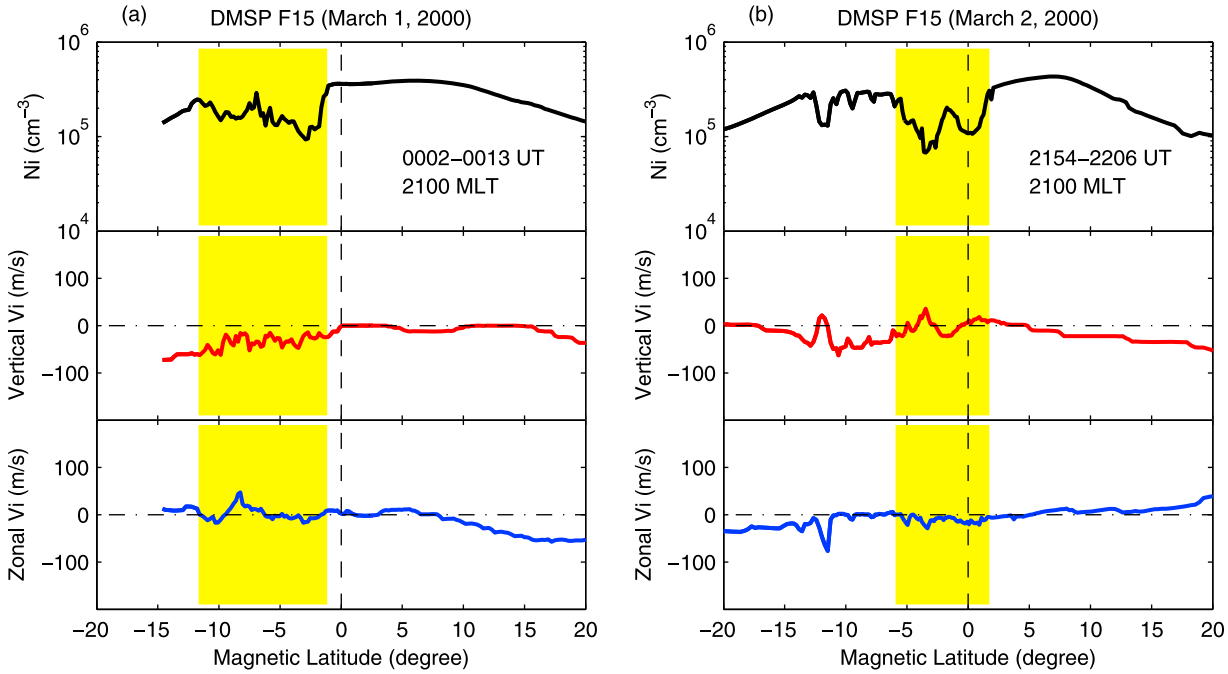

Figure 3. Examples of dead plasma bubbles. From top to bottom are the ion density, ion vertical velocity, and ion zonal velocity measured by the DMSP F15 satellite on (a) 1 March and (b) 2 March 2000. The ion zonal drift inside the density depletion region is very close to the ambient plasma drift.

of the ion drifts are measured by both the ROCSAT-1 and DMSP satellites.

[17] The plasma depletions presented in Figures 1–4 are detected in the evening sector during the last solar maximum. ROCSAT-1 observations show that the occurrence probability of equatorial plasma bubbles and density irregularities over the period of 1999–2004 peaks at ~2100 LT and reduces toward the dawn sector [*Su et al.*, 2009]. The C/NOFS satellite was launched in April 2008 to forecast ambient plasma densities and irregularities in the equatorial ionosphere [*de La Beaujardière et al.*, 2004]. Instruments on C/NOFS measure electric fields, plasma characteristics, neutral winds, and the strength of scintillation-producing irregularities in the low-latitude ionosphere. An unexpected feature revealed by the C/NOFS measurements is the presence of deep plasma depletions in the midnight-dawn sector at all satellite altitudes [*de La Beaujardière et al.*, 2009]. Note that the ionospheric conditions can be significantly different during solar maximum and minimum. The plasma bubbles detected by the DMSP and ROCSAT-1 satellites occurred in the evening sector, and the plasma bubbles detected by C/NOFS occurred in the midnight-dawn sector. The C/NOFS measurements are used to show the characteristics of the plasma bubble zonal drift in the midnight-dawn sector but not to compare with the measurements of the DMSP and ROCSAT-1 satellites.

[18] Figure 5 shows the plasma depletions measured by the C/NOFS satellite in the postmidnight sector on 2 and 6 June 2008. The ion density is measured by the Planar Langmuir Probe, and the electric fields are measured by the Vector Electric Field Instrument (VEFI). The density and electric field data have a time resolution of 1 s. An important feature of the postmidnight plasma depletions is that the electric fields inside the depletion regions are significantly enhanced, as denoted by the shadings. The zonal electric field inside the depletions is eastward, and the corresponding $\mathbf{E} \times \mathbf{B}$ drift is in the meridional/upward direction. We have calculated the $\mathbf{E} \times \mathbf{B}$ drift velocities from the electric field, and the velocities are plotted in Figures 5d–5e and 5I–5j for the two cases, respectively. The upward drift velocity inside the depletions is 100–300 m s^{-1}, implying that these post-midnight depletions are plasma bubbles, which are rising very fast. The meridional electric field corresponds to the $\mathbf{E} \times \mathbf{B}$ drift in the zonal direction. The zonal drift velocity outside the depletion regions is mostly positive, indicating that the ambient plasma is drifting eastward. The zonal drift velocity inside the depletions is negative, showing that the plasma particles inside the bubbles are drifting westward.

[19] Figure 6 presents two cases in which the zonal drifts show more complicated characteristics. In the case of 5 June 2008 (the left column of Figure 6), the ambient plasma is slowly drifting westward, and the plasma particles inside the first three depletions between 2337 and 2339 UT are drifting westward at a speed faster than the ambient plasma drift. Inside the depletion at 2340 UT, the maximum upward velocity is 360 m s^{-1}, and the zonal drift velocity there becomes eastward. In the case of 9 June 2008 (the right column of Figure 6), the maximum upward velocity inside the depletion reaches 380 m s^{-1} at 0216 UT, and the zonal drift velocity changes between eastward and westward several times. The observations imply that the spacecraft enters regions with alternately eastward and westward plasma flow.

[20] Finally, we present the simulation results of ion drift velocities during ESF process. In most of previous numerical simulations of ESF, only the density structures of plasma bubbles were analyzed. A new simulation with a 3-D

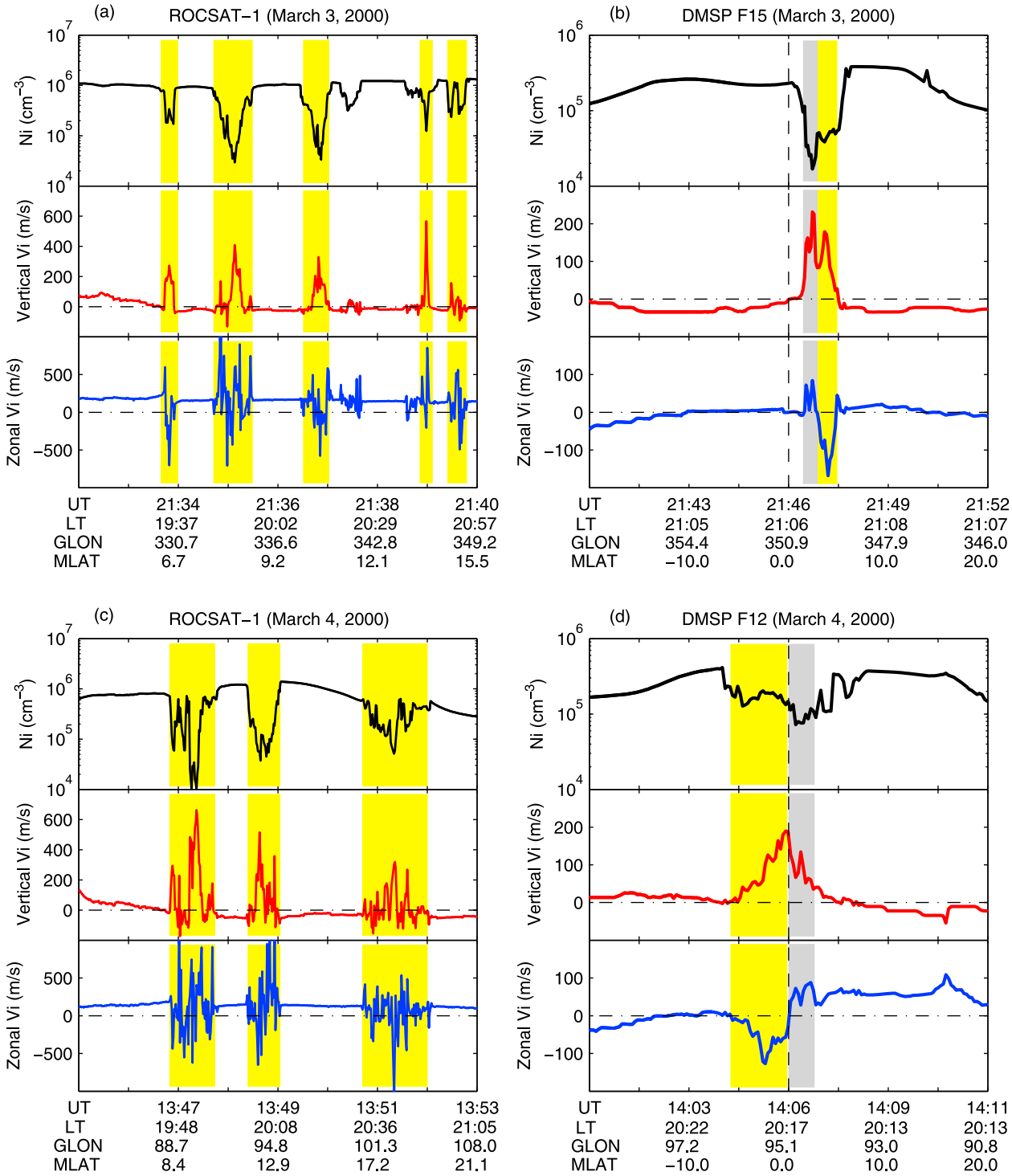

Figure 4. Comparison of the ion density depletions and drift velocities measured by the ROCSAT-1 and DMSP satellites nearly simultaneously on (a–b) 3 March and (c–d) 4 March 2000.

model concentrates on the drift velocities inside and outside plasma bubbles. The detailed calculations and evolution of the plasma bubbles are given in the study of *Retterer* [2010]. In Figure 7, we only show two snapshots of the spatial distribution of the ion drift velocities in the evening sector while plasma bubbles develop. Figures 7a–7b show the ion vertical velocity. At 2032 LT, the bubble at 300 km to the west has reached 800 km in altitude and bifurcated, and another bubble at 150 km to the west has reached 450 km in altitude. By 2136 LT, the two bubbles have drifted east by ~300 km, the bubble on the left has reached 1000 km in altitude, and the bubble on the right has reached 800 km in altitude. The vertical velocity inside the bubbles is upward, indicating that the bubbles are still rising. The vertical velocity of the

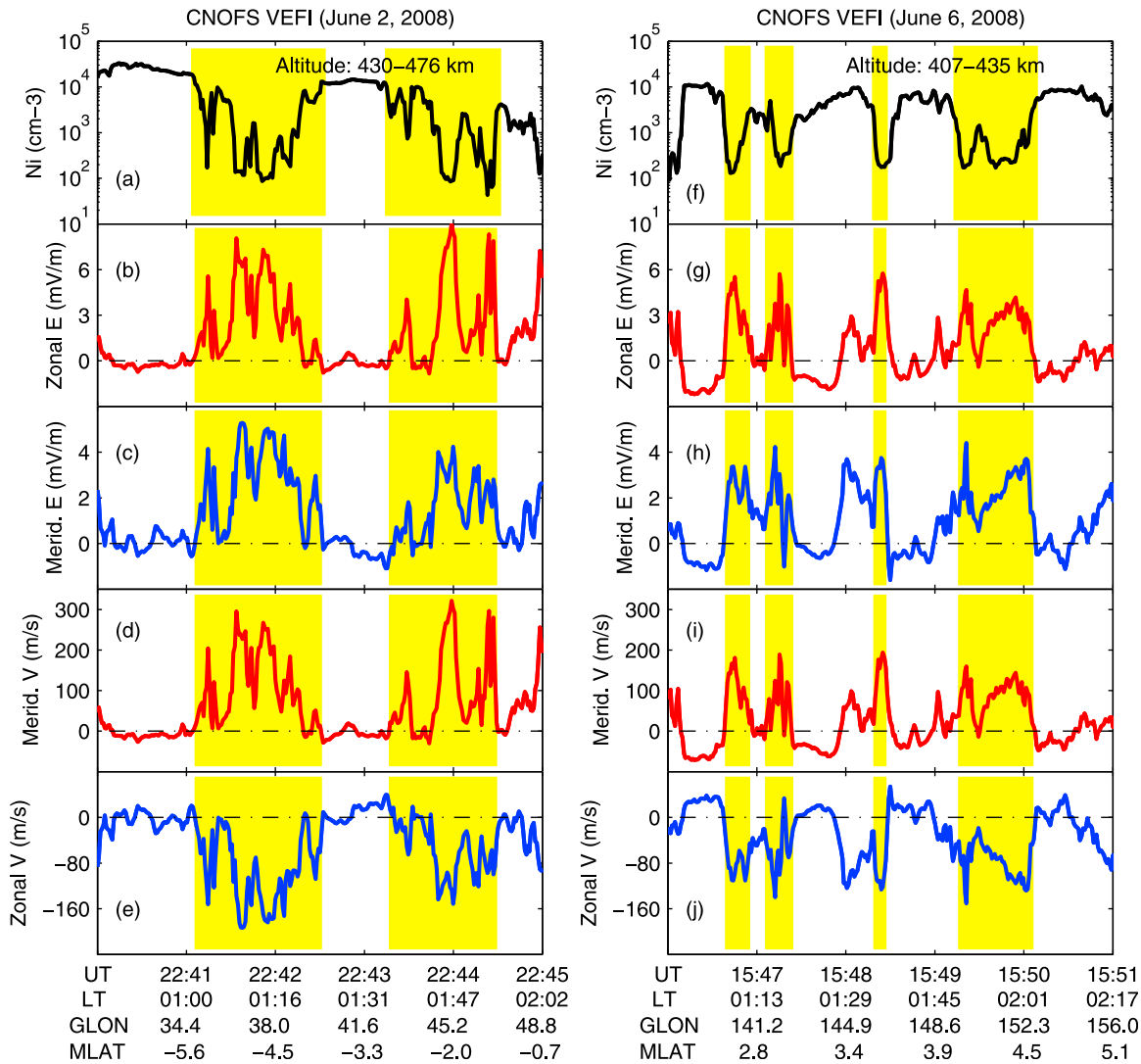

Figure 5. Plasma depletions measured by the C/NOFS satellite in the postmidnight sector. From Figure 5a to 5e are the ion density, zonal electric field, meridional electric field, meridional drift velocity, and zonal drift velocity on 2 June 2008. (f–j) Same as Figures 5a–5e but for 6 June 2008.

ambient plasma is slightly negative, implying that the ambient plasma moves slowly downward.

[21] The zonal drift velocity in Figures 7c–7d shows very interesting characteristics. The ambient plasma drifts eastward. The plasma bubble on the left in Figure 7c shows a reversed C shape. The lower portion of the bubble (below 400 km in altitude) is tilted to the east, and the ions inside this portion of the bubble drift eastward at a speed larger than the ambient plasma drift. The main stem of the bubble above 400 km is tilted to the west, and the zonal drift velocity of the ions inside it is westward. A major branch of the bubble is tilted to the east in the altitude range of 560–660 km, and the zonal drift velocity of the ions within this branch is eastward. At later time, as shown in Figure 7d, the lower portion of the bubbles (below 320 km) is tilted to the east, and the ion zonal drift velocity is eastward there. Above 320 km, the plasma bubbles, including their major branches, are tilted to the west, and the ion zonal drift velocity is westward. The important phenomenon manifested by the simulations is that the ion zonal drift inside the depletion region is eastward if the depletion is tilted to the east and westward if the depletion is tilted to the west.

3. Discussion

[22] Equatorial ionospheric plumes/bubbles often show an arc structure like a reversed C shape [*Woodman and La Hoz*, 1976; *Kelley et al.*, 1981]. The lower portion of equatorial plasma bubbles often tilts eastward, and the upper portion tilts westward. It has been suggested that the reversed C shape of the bubble structure is caused by the shear in neutral wind and ionospheric Pedersen conductivity [*Zalesak et al.*, 1982]. The numerical simulations in Figure 7 reproduce the arc structure and show that the direction of the zonal drift of the plasma particles inside depletions depends on the orientation of the depletion structure. The observations of the DMSP, ROCSAT-1, and C/NOFS satellites show that the zonal drift

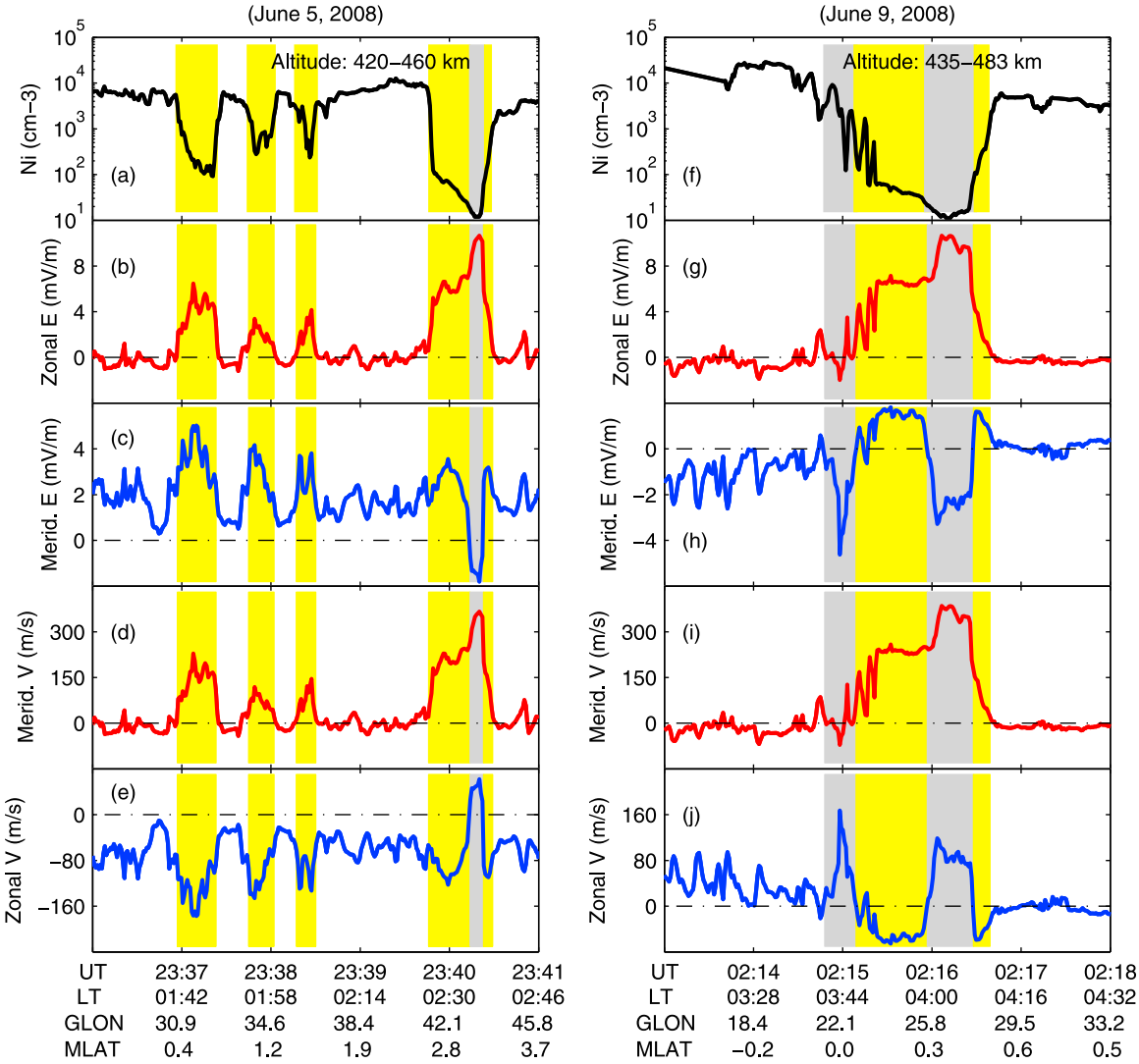

Figure 6. Plasma depletions measured by the C/NOFS satellite in the postmidnight sector. From Figure 6a to 6e are the ion density, zonal electric field, meridional electric field, meridional drift velocity, and zonal drift velocity on 5 June 2008. (f–j) Same as Figures 6a–6e but for 9 June 2008. The zonal drift velocity inside the depletions show complicated characteristics.

velocity of the plasma particles inside the depletion regions can be eastward and/or westward.

[23] Here we suggest the following mechanism that can cause the observed characteristics of the ion zonal drift velocity. Inside a plasma bubble, polarization electric field is generated, and this polarization electric field is directed from the west to the east wall [*Ossakow and Chaturvedi*, 1978; *Huang and Kelley*, 1996a]. If the bubble is upright, the polarization electric field is eastward and drives upward drift of plasma particles. However, both observations and simulations show that plasma bubbles/plumes are often tilted. The polarization electric field inside a tilted plasma bubble is perpendicular to the axis of the bubble.

[24] Figure 8 illustrates the electric fields and plasma drifts inside plasma bubbles. The yellow background represents the ambient plasma that drifts eastward, and the white regions represent plasma bubbles. In Figure 8a, two plasma bubbles are depicted. The simple bubble without bifurcation on the left is tilted to the west. Because of the tilt of the bubble, the polarization electric field has two components: one is in the eastward direction and the other is in the upward direction. The bifurcated bubble on the right has two branches. The electric field inside the west-tilted branch has an eastward component and an upward component. In contrast, the electric field inside the east-tilted branch has an eastward component and a downward component.

[25] The polarization electric field drives the $\mathbf{E} \times \mathbf{B}$ drift of the plasma particles inside the bubble. The geomagnetic field in the equatorial region is approximately horizontal and directed toward north. The eastward electric field causes an upward drift, the upward electric field causes a westward drift, and the downward electric field causes an eastward drift. The $\mathbf{E} \times \mathbf{B}$ drift of the plasma particles inside the bubble is depicted in Figure 8b. The zonal component of the $\mathbf{E} \times \mathbf{B}$ drift velocity is westward in the west-tilted bubble but eastward in the east-tilted bubble. *Aggson et al.* [1992, 1996] and *Laakso et al.* [1994, 1997] presented the observations of electric fields inside equatorial plasma bubbles. Our inter-

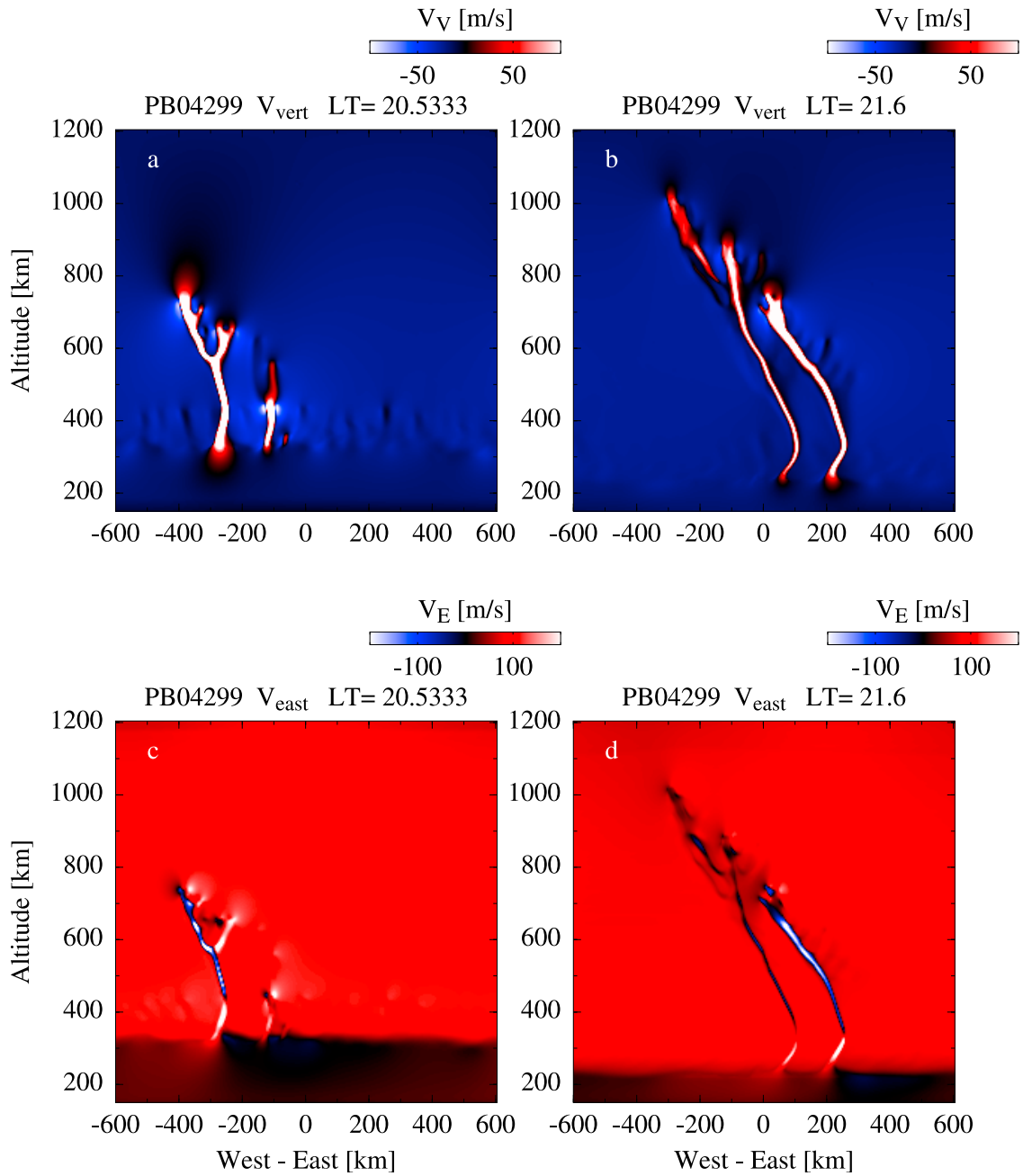

Figure 7. Three-dimensional simulation results of plasma velocities during equatorial spread *F*. The top panels show the ion vertical velocity, and the bottom panels show the ion zonal velocity.

pretation is consistent with their results and with the simulations in Figure 7.

[26] We now explain the spacecraft measurements of the ion zonal drift velocities inside plasma bubbles. If a spacecraft flies across the west-tilted bubble, as the one depicted on the left of Figure 8b, it will detect an upward velocity and a westward velocity. If the spacecraft flies across the bifurcated bubble, as the one depicted on the right of Figure 8b, the ion zonal velocity detected by the spacecraft will be first westward and then eastward (depending on the spacecraft orbit). If the structure of the plasma bubble is more complicated and has multiple branches, a spacecraft will detect alternately westward-eastward velocities. Similarly, the meridional/vertical electric field measured by the spacecraft (such as C/NOFS) will show positive-negative variations in bifurcated plasma bubbles.

[27] The next issue we want to address is how the zonal drift velocity of the plasma particles inside a plasma bubble is related to the drift of the bubble structure. *McClure et al.* [1977] analyzed the plasma drifts measured by the Atmosphere Explorer satellite. They found irregular upward and westward motion of the order of 150 m s^{-1} associated with some of equatorial plasma bubbles, while others moved more slowly or moved with approximately the velocity of the background plasma. Subsequent observations show that the equatorial depletions drift eastward, especially in the

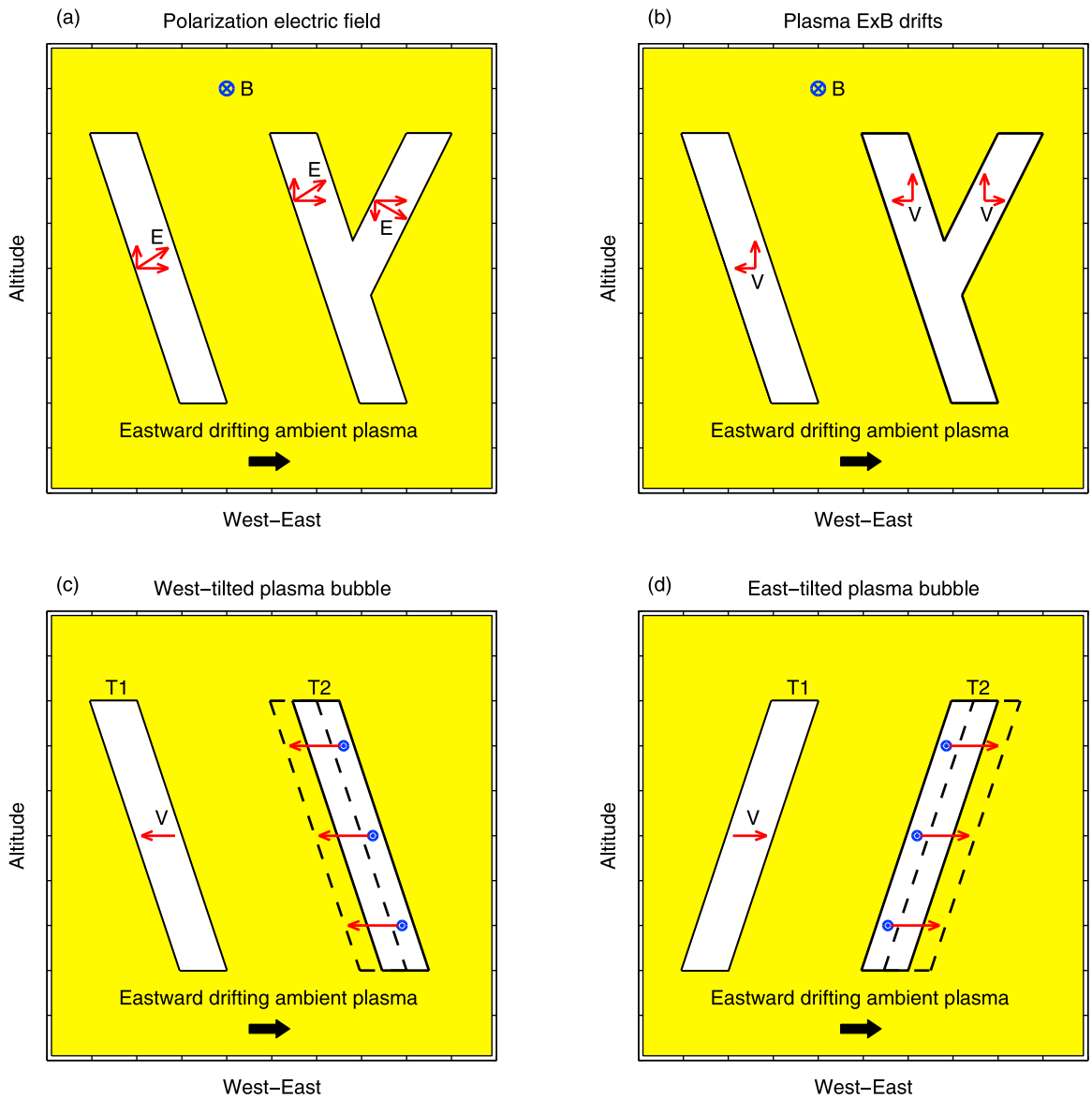

Figure 8. (a–b) Illustration of the polarization electric field and **E** × **B** drift velocity inside plasma density depletions. (c–d) Illustration of the contribution of the zonal **E** × **B** drift inside the depletion region to the zonal drift of the bubble structure.

evening sector [*Abdu et al.*, 1985, 2003; *Valladares et al.*, 1996; *Taylor et al.*, 1997; *Sobral et al.*, 1999; *Bhattacharyya et al.*, 2001; *Immel et al.*, 2003, 2004; *Lin et al.*, 2005; *Park et al.*, 2007]. However, no simultaneous measurement of the background plasma drift was made in most experiments. Some investigators found that the zonal drift of plasma depletions could be higher than the average *F* region plasma zonal drift.

[28] We suggest that the difference between the zonal drift of plasma depletions and the ambient plasma drift can be caused by the motion of the plasma particles inside the depletion region. In Figure 8c, a west-tilted plasma bubble is depicted. The ambient plasma is assumed to drift eastward. The plasma bubble at time T_1 is in the location on the left. If we assume that the structure of the plasma bubble drifts with the ambient plasma, the bubble will reach the location denoted by the dashed lines at a later time T_2. However, because the zonal drift velocity of the plasma particles inside the bubble is westward, it implies that the plasma particles move away from the east wall and then pile up on the west wall. It can be seen in Figure 1 that the westward velocity of the plasma particles is the largest at the center of the depletion region and reduces toward the boundary of the depletion. The zonal drift velocity of the plasma particles inside the depletion becomes the same as the zonal drift of the ambient plasma at the edge of the depletion. In other words, the plasma particles inside the depletion and the ambient plasma have the same zonal drift at the west wall of the depletion, so the plasma particles pile up there. As a consequence, the real location of the bubble will be the one depicted by the solid lines and is to the east of that denoted by the dashed lines. In other words, the plasma bubble has reached a location to the east of a bubble that was assumed to drift with the ambient

plasma. Therefore, the zonal drift velocity of the plasma bubble structure is faster than the ambient plasma drift.

[29] Equatorial plasma bubbles are, in general, generated in the evening sector after the *F* region is moved to higher altitudes by the prereversal enhancement. During the initial phase of bubble development, the bubbles are moving upward. The DMSP measurements in the evening sector show that the ion vertical velocity inside depletion regions is upward, consistent with rising bubbles. Because most plasma bubbles are tilted westward, the plasma zonal drifts driven by the polarization electric field inside the bubbles are westward. As illustrated in Figure 8c, the westward motion of the plasma particles inside the bubbles causes the bubble structure to move faster than the ambient plasma drift.

[30] Observations also show that the zonal drift of the bubble structure can be slower than the average *F* region plasma drift [*Bhattacharyya et al.*, 2001], which can be explained by the zonal drift of the plasma particles inside east-tilted bubbles. An east-tilted plasma bubble is illustrated in Figure 8d. In this case the ambient plasma drifts eastward, and the plasma particles inside the bubble also drift eastward. The plasma particles move away from the west wall of the bubble and pile up on the east wall. Consequently, the eastward drift velocity of the bubble structure is slower than the ambient plasma drift.

[31] In the scenario proposed above, the eastward drift velocity of the bubble structure is faster than the ambient plasma drift if the bubble is tilted westward and slower than the ambient plasma drift if the bubble is tilted eastward. Because plasma bubbles are found to be tilted westward in most radar measurements, it is expected from this scenario that the eastward drift velocity of the bubble structure is generally faster than the average *F* region plasma drift. Although the mechanism depicted in Figures 8c–8d cannot be directly confirmed with the data presented in this paper, the interpretation is consistent with the observations [*Valladares et al.*, 1996; *Bhattacharyya et al.*, 2001; *Immel et al.*, 2003; *Lin et al.*, 2005].

[32] If a plasma bubble is no longer moving upward, it may be termed a dead bubble. The polarization electric field inside the dead bubble becomes negligible and does not cause noticeable plasma particle drifts relative to the ambient plasma. As can be seen in the DMSP measurements of Figure 3, the relative drift velocity of the plasma particles inside the depletion region with respect to the ambient plasma is small or nearly zero. Therefore, the zonal drift of the dead bubble structure is nearly the same as the ambient plasma drift. The polarization electric field inside plasma bubbles can be strong during the initial phase of bubble development but becomes very weak at the end of the bubble life. If a plasma bubble is generated in the evening sector, this bubble may become a dead bubble after it drifts into the postmidnight sector. Observations show that the zonal drift velocity of plasma bubbles becomes closer to the average *F* region plasma drift at later local times [*Bhattacharyya et al.*, 2001].

[33] However, the plasma bubbles in the postmidnight sector are not necessarily dead bubbles. In fact, the C/NOFS satellite has detected the frequent occurrence of deep plasma depletions in the midnight-dawn sector during the solar minimum years (2008–2009), such as the examples presented in Figures 5–6. In these cases, the electric fields inside the depletion regions are much stronger than those in the ambient plasma and can be reasonably explained to be the polarization electric field. The corresponding $\mathbf{E} \times \mathbf{B}$ drift velocities of the plasma particles driven by the polarization electric field inside the bubbles are upward and westward and reach 200–400 m s^{-1}, indicating that the postmidnight plasma bubbles are active and still growing.

[34] In the context of this paper's findings, we are still left with the following challenges to explain the C/NOFS observations. (1) If the plasma bubbles detected by C/NOFS originated in the evening sector and have drifted several hours to reach the postmidnight sector, why is the polarization electric field inside the bubbles still very strong during this late period of the bubble? (2) Radar and satellite observations have shown that the vertical plasma drift is generally upward in the evening sector and downward in the postmidnight sector [*Fejer et al.*, 1991, 2008]. However, C/NOFS frequently detected plasma bubbles in the midnight-dawn sector but not in the evening sector during 2008–2009. The plasma bubbles were detected during quiet times, no significant geomagnetic disturbance (magnetic storm) occurred. We also checked the DMSP measurements in the evening sector and found very few bubbles there. Why do plasma bubbles often occur in the postmidnight sector but not in the evening sector? (3) If the plasma bubbles are generated in the midnight-dawn sector, the equatorial *F* region must have been moved to higher altitudes for the generation of the bubbles. What causes the upward plasma drift in the postmidnight equatorial ionosphere during the solar minimum years? Is the plasma drift during this solar minimum different from the average patterns derived from previous solar minima? Further investigations are required to solve these outstanding problems.

4. Conclusions

[35] We have presented measurements of ion drift velocities by the DMSP, ROCSAT-1, and C/NOFS satellites associated with equatorial plasma bubbles. Our analysis focuses on the ion zonal drift inside plasma bubbles and its relation to the zonal drift of the bubble structure. The conclusions derived from this study are as follows.

[36] The zonal drift velocity of the plasma particles inside plasma bubbles is significantly different from the ambient plasma drift in the evening sector. In the 530 cases of depletions detected by the DMSP satellites in January–March 2000, the relative zonal drift velocity of ions inside the depletion region with respect to the ambient plasma is westward in 75% cases, small or near zero in 19% cases, and eastward in 6% cases. The zonal drift velocity within the depletions can be several hundreds of meters per second.

[37] The drift velocity of the plasma inside the depletion region is driven by the polarization electric field. When a plasma bubble is tilted, the polarization electric field has a zonal component and a vertical component. The zonal electric field causes the upward drift velocity, and the vertical electric field causes the zonal drift velocity.

[38] The zonal drift velocity of the bubble structure is different from the ambient plasma drift because of the zonal motion of the plasma particles inside the bubble. The eastward drift velocity of the bubble structure is faster than the ambient plasma drift if the bubble is tilted westward and

slower than the ambient plasma drift if the bubble is tilted eastward. Because plasma bubbles are mostly tilted westward, the zonal drift velocity of the bubble structure is expected to be generally faster than the average *F* region plasma drift.

[39] The C/NOFS satellite frequently detects plasma depletions in the midnight-dawn sector. The polarization electric field inside the depletions is much stronger than the electric field in the ambient plasma, and the postmidnight depletions are rising plasma bubbles. It is still not well understood what causes the frequent occurrence of the postmidnight bubbles during the solar minimum years (2008–2009). This requires further investigations.

[40] **Acknowledgments.** Work by C.S.H. was supported by the Air Force Office of Scientific Research (AFOSR) award FA9550-09-1-0321. The C/NOFS mission is supported by the Air Force Research Laboratory, the Department of Defense Space Test Program, NASA, the Naval Research Laboratory, and The Aerospace Corporation. We thank Eftyhia Zesta for helpful discussion on the DMSP VEFI data. We gratefully acknowledge the Air Force Research Laboratory for providing the DMSP thermal plasma data.

[41] Robert Lysak thanks Jose Sobral and Marc Hairston for their assistance in evaluating this paper.

References

Abdu, M., I. Batista, J. Sobral, E. de Paula, and I. Kantor (1985), Equatorial ionospheric plasma bubble irregularity occurrence and zonal velocities under quiet and disturbed conditions, from polarimeter observations, *J. Geophys. Res.*, *90*(A10), 9921–9928.

Abdu, M. A., I. S. Batista, H. Takahashi, J. MacDougall, J. H. Sobral, A. F. Medeiros, and N. B. Trivedi (2003), Magnetospheric disturbance induced equatorial plasma bubble development and dynamics: A case study in Brazilian sector, *J. Geophys. Res.*, *108*(A12), 1449, doi:10.1029/2002JA009721.

Aggson, T. L., H. Laakso, N. C. Maynard, and R. F. Pfaff (1996), In situ observations of bifurcation of equatorial ionospheric plasma depletions, *J. Geophys. Res.*, *101*(A3), 5125–5132.

Aggson, T. L., N. C. Maynard, W. B. Hanson, and J. L. Saba (1992), Electric Field Observations of Equatorial Bubbles, *J. Geophys. Res.*, *97*(A3), 2997–3009.

Bhattacharyya, A., S. Basu, K. M. Groves, C. E. Valladares, and R. Sheehan (2001), Dynamics of equatorial *F* region irregularities from spaced receiver scintillation observations, *Geophys. Res. Lett.*, *28*(1), 119–122.

de La Beaujardière, O., et al. (2004), C/NOFS: A mission to forecast scintillations, *J. Atmos. Sol. Terr. Phys.*, *66*, 1573–1591, doi:10.1016/j.jastp.2004.07.030

de La Beaujardière, O., et al. (2009), C/NOFS observations of deep plasma depletions at dawn, *Geophys. Res. Lett.*, *36*, L00C06, doi:10.1029/2009GL038884.

Fejer, B. G., E. R. de Paula, S. A. González, and R. F. Woodman (1991), Average vertical and zonal *F* region plasma drifts over Jicamarca, *J. Geophys. Res.*, *96*(A8), 13, 901–913, 906.

Fejer, B. G., J. R. Souza, A. S. Santos, and A. E. Costa Pereira (2005), Climatology of region zonal plasma drifts over Jicamarca, *J. Geophys. Res.*, *110*, A12310, doi:10.1029/2005JA011324.

Fejer, B. G., J. W. Jensen, and S.-Y. Su (2008), Quiet time equatorial region vertical plasma drift model derived from ROCSAT-1 observations, *J. Geophys. Res.*, *113*, A05304, doi:10.1029/2007JA012801.

Huang, C.-S., and M. C. Kelley (1996a), Nonlinear evolution of equatorial spread *F*. 1. On the role of plasma instabilities and spatial resonance associated with gravity wave seeding, *J. Geophys. Res.*, *101*(A11), 283–292.

Huang, C.-S., and M. C. Kelley (1996b), Nonlinear evolution of equatorial spread *F*. 2. Gravity wave seeding of Rayleigh-Taylor instability, *J. Geophys. Res.*, *101*(A11), 293–302.

Huang, C.-S., and M. Kelley (1996c), Nonlinear evolution of equatorial spread *F* 3. Plasma bubbles generated by structured electric fields, *J. Geophys. Res.*, *101*(A1), 303–313.

Huba, J. D., G. Joyce, and J. Krall (2008), Three-dimensional equatorial spread *F* modeling, *Geophys. Res. Lett.*, *35*, L10102, doi:10.1029/2008GL033509.

Immel, T. J., S. B. Mende, H. U. Frey, L. M. Peticolas, and E. Sagawa (2003), Determination of low latitude plasma drift speeds from FUV images, *Geophys. Res. Lett.*, *30*(18), 1945, doi:10.1029/2003GL017573.

Immel, T., H. Frey, S. Mende, and E. Sagawa (2004), Global observations of the zonal drift speed of equatorial ionospheric plasma bubbles, *Ann. Geophys.*, *22*, 3099–3107.

Kelley, M. C., M. F. Larsen, C. LaHoz, and J. P. McClure (1981), Gravity wave initiation of equatorial spread *F*: A case study, *J. Geophys. Res.*, *86*(A11), 9087–9100.

Keskinen, M. J., S. L. Ossakow, and B. G. Fejer (2003), Three-dimensional nonlinear evolution of equatorial ionospheric spread *F* bubbles, *Geophys. Res. Lett.*, *30*(16), 1855, doi:10.1029/2003GL017418.

Laakso, H., T. L. Aggson, R. F. Pfaff, and W. B. Hanson (1994), Downdrafting Plasma Flow in Equatorial Bubbles, *J. Geophys. Res.*, *99*(A6), 11,507–11,515.

Laakso, H., N. C. Maynard, R. F. Pfaff, T. L. Aggson, W. R. Coley, P. Janhunen, and F. A. Herrero (1997), Electric field diagnostics of the dynamics of equatorial density depletions, *J. Atmos. Sol. Terr. Phy.*, *59*(13), 1625–1631.

Lin, C. S., T. J. Immel, H.-C. Yeh, S. B. Mende, and J. L. Burch (2005), Simultaneous observations of equatorial plasma depletion by IMAGE and ROCSAT-1 satellites, *J. Geophys. Res.*, *110*, A06304, doi:10.1029/2004JA010774.

McClure, J., W. Hanson, and J. Hoffman (1977), Plasma bubbles and irregularities in the equatorial ionosphere, *J. Geophys. Res.*, *82*(19), 2650–2656.

Ossakow, S. L., and P. K. Chaturvedi (1978), Morphological studies of rising equatorial spread *F* bubbles, *J. Geophys. Res.*, *83*(A5), 2085–2090.

Park, S. H., S. L. England, T. J. Immel, H. U. Frey, and S. B. Mende (2007), A method for determining the drift velocity of plasma depletions in the equatorial ionosphere using far ultraviolet spacecraft observations, *J. Geophys. Res.*, *112*, A11314, doi:10.1029/2007JA012327.

Retterer, J. M. (2010), Forecasting low-latitude radio scintillation with 3-D ionospheric plume models: 1. Plume model, *J. Geophys. Res.*, *115*, A03306, doi:10.1029/2008JA013839.

Retterer, J. M., R. Ilma, M. C. Kelley, J. L. Chau, C. E. Valladares, L. C. Gentile, and K. Groves (2009), Modeling the low-latitude ionospheric electron density and plasma turbulence in the November 2004 storm period, *J. Atmos. Sol.-Terr. Phys.*, doi:10.1016/j.jastp.2009.07.012.

Rich, F. J., and M. Hairston (1994), Large-scale convection patterns observed by DMSP, *J. Geophys. Res.*, *99*(A3), 3827–3844.

Scannapieco, A. J., and S. L. Ossakow (1976), Nonlinear spread *F*, *Geophys. Res. Lett.*, *3*, 451–454.

Sobral, J. H. A., M. A. Abdu, H. Takahashi, H. Sawant, C. J. Zamlutti, G. L. Borba (1999), Solar and geomagnetic activity effects on nocturnal zonal velocities of ionospheric plasma depletions, *Adv. Space Res.*, *24*(11), 1507–1510.

Su, S.-Y., C. K. Chao, and C. H. Liu (2009), Cause of different local time distribution in the postsunset equatorial ionospheric irregularity occurrences between June and December solstices, *J. Geophys. Res.*, *114*, A04321, doi:10.1029/2008JA013858.

Taylor, M. J., J. V. Eccles, J. LaBelle, and J. H. A. Sobral (1997), High resolution OI (630 nm) image measurements of *F* region depletion drifts during the Guará Campaign, *Geophys. Res. Lett.*, *24*(13), 1699–1702.

Valladares, C., R. Sheehan, S. Basu, H. Kuenzler, and J. Espinoza (1996), The multi-instrumented studies of equatorial thermosphere aeronomy scintillation system: Climatology of zonal drifts, *J. Geophys. Res.*, *101*(A12), 26,839–26,850.

Woodman, R. F., and C. La Hoz (1976), Radar observations of *F* region equatorial irregularities, *J. Geophys. Res.*, *81*(31), 5447–5466.

Yokoyama, T., S. Fukao, and M. Yamamoto (2004), Relationship of the onset of equatorial region irregularities with the sunset terminator observed with the Equatorial Atmosphere Radar, *Geophys. Res. Lett.*, *31*, L24804, doi:10.1029/2004GL021529.

Zalesak, S., S. Ossakow, and P. Chaturvedi (1982), Nonlinear equatorial spread *F*: The effect of neutral winds and background Pedersen conductivity, *J. Geophys. Res.*, *87*(A1), 151–166.

O. de La Beaujardiere, D. E. Hunton, J. M. Retterer, P. A. Roddy, and Y.-J. Su, Space Vehicles Directorate, Air Force Research Laboratory, 29 Randolph Road, Hanscom AFB, MA 01731, USA.

C.-S. Huang, Boston College, Institute for Scientific Research, 402 St Clement's Hall, 140 Commonwealth Avenue, Chestnut Hill, MA 02467, USA. (chaosong.huang.ctr@hanscom.af.mil)

R. F. Pfaff, NASA Goddard Space Flight Center, Mail Code 674, Greenbelt, MD 20771, USA.

F. J. Rich, Lincoln Laboratory, Massachusetts Institute of Technology, Group 97, 244 Wood Street, Lexington, MA 02421, USA.

S.-Y. Su, Institute of Space Science and Center for Space and Remote Sensing Research, National Central University, Chung-Li 32054, Taiwan.